IEICE TRANSACTIONS

on Electronics

VOL. E98-C NO. 5
MAY 2015

A PUBLICATION OF THE ELECTRONICS SOCIETY

The Institute of Electronics, Information and Communication Engineers
Kikai-Shinko-Kaikan Bldg., 5-8, Shibakoen 3 chome, Minato-ku, TOKYO, 105-0011 JAPAN

IEICE TRANS. ELECTRON., VOL.E98–C, NO.5 MAY 2015

PAPER Special Section on Fundamentals and Applications of Advanced Semiconductor Devices

Analysis on Non-Ideal Nonlinear Characteristics of Graphene-Based Three-Branch Nano-Junction Device

Xiang YIN[†], *Nonmember*, **Masaki SATO**[†], *Student Member*, *and* **Seiya KASAI**[†a)], *Member*

SUMMARY We investigate the origin of non-ideal transfer characteristics in graphene-based three-branch nano-junction (TBJ) devices. Fabricated graphene TBJs often show asymmetric nonlinear voltage transfer characteristic, although symmetric one should appear ideally. A simple model considering the contact resistances in two input electrodes is deduced and it suggests that the non-ideal characteristic arises from inequality of the metal-graphene contact resistances in the inputs. We fabricate a graphene TBJ device with electrically equal contacts by optimizing the contact formation process and almost ideal nonlinear characteristic was successfully demonstrated.

key words: *graphene, TBJ, nonlinear characteristic, contact resistance, graphene-metal contact*

1. Introduction

A three-branch nano-junction (TBJ) is a T or Y-shaped tinny three-terminal device. It exhibits unique nonlinear voltage transfer characteristic [1]. This makes a TBJ device, in case with electron carriers, to operate as a two-input AND gate [2], [3]. Graphene is very attractive material for the TBJ, since the polarity of the nonlinear curve can be switched by electric field effect owing to ambipolar transport [4], [5] together with high carrier mobility at room temperature (RT). This suggests that the graphene TBJ can operate as not only AND gate but also OR gate [5]. Furthermore, we recently demonstrated that the graphene TBJ could also operate as a NOT gate [6]. Therefore the graphene has a potential to implement a complete set of logic gates by itself. However, voltage transfer characteristics in the fabricated devices often deviated from the ideal one [4], [6], [8], which deteriorates the logic gate operations. In this paper, we investigate the origin of the non-ideal voltage transfer characteristics in the graphene TBJs. A simple equivalent circuit model is deduced to explain the observed behavior and we point out the effect of metal-graphene contact resistance inequality. Then we experimentally demonstrate that an ideal nonlinear curve can be achieved by forming equal contacts of the two inputs using an optimized metal-graphene contact formation process.

Manuscript received September 9, 2014.
Manuscript revised December 12, 2014.

[†]The authors are with Research Center for Integrated Quantum Electronics and Graduate School of Information Science and Technology, Hokkaido University, N13, W8, Sapporo 060-8628, Japan.
a) E-mail: kasai@rciqe.hokudai.ac.jp

DOI: 10.1587/transele.E98.C.434

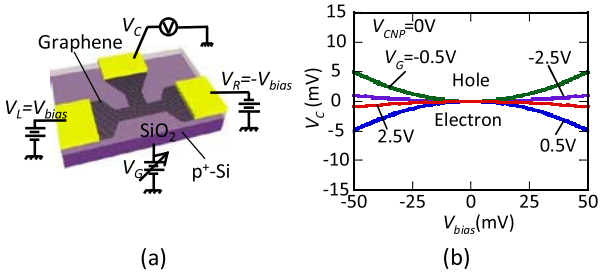

Fig. 1 (a) Schematic of a graphene TBJ and (b) ideal voltage transfer characteristics.

2. Theoretical Model

Basic structure of a graphene-based TBJ together with typical measurement setup is shown in Fig. 1(a). The TBJ has two input branches and an output branch. A back gate controls the carriers in graphene. When the left and right branches are biased in push–pull fashion, $V_{\mathrm{L}} = V_{\mathrm{bias}}$ and $V_{\mathrm{R}} = -V_{\mathrm{bias}}$, the center branch voltage V_{C} as a function of V_{bias} shows a parabolic curve as shown in Fig. 1(b) [7]. The curvature and polarity of curves can be changed by gate voltage V_{G}, since they depend on carrier density and conduction type, respectively. The basic behavior can be described by an input-electrode capacitor model [6], [7], where the conductance in the two input branches are unequal due to the difference in the induced charge density underneath the two input electrodes. However, experimental curves often obviously incline to left or right. This non-ideal behavior has been considered to arise from the inequality of the contact resistance of the inputs [6].

To understand the observed non-ideal behavior, we consider an equivalent circuit model including the input contact resistances as shown in Fig. 2. In this model, V_{C} is simply expressed by

$$V_{\mathrm{C}} = \frac{(R_{-} + R_{\mathrm{C}-}) - (R_{+} + R_{\mathrm{C}+})}{(R_{-} + R_{\mathrm{C}-}) + (R_{+} + R_{\mathrm{C}+})} V_{\mathrm{bias}}, \tag{1}$$

where R_{-} and R_{+} are resistance values of the negatively and positively biased input branches, and $R_{\mathrm{C}-}$ and $R_{\mathrm{C}+}$ are metal-graphene contact resistance values in the negatively and positively biased input electrodes, respectively. R_{-} and R_{+} are evaluated by the next formulas,

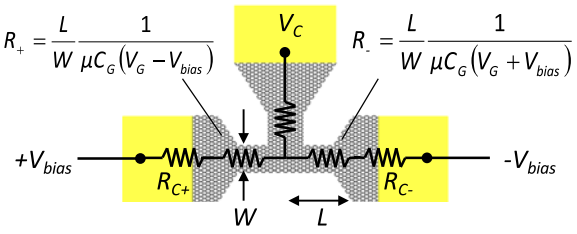

Fig. 2 Equivalent circuit model including contact resistance in the two inputs.

$$R_- = \frac{L}{W}\frac{1}{\mu C_G(V_G + V_{bias})},$$
$$R_+ = \frac{L}{W}\frac{1}{\mu C_G(V_G - V_{bias})} \quad (2)$$

where L and W is the input branch length and width, respectively, C_G is gate capacitance, and μ is mobility. Here the charge neutrality point of graphene V_{CNP} is assumed to be 0 V. When $V_{bias} \ll V_G$, Eq. (1) is approximately given by the next formula,

$$V_C \approx -\frac{2}{V_G[2+kV_G(R_{C+}+R_{C-})]}V_{bias}^2 + \frac{k(R_{C-}-R_{C+})V_G}{2+kV_G(R_{C+}+R_{C-})}V_{bias} \quad (3)$$

where $k = \mu C_G W/L$. In case of $R_{C+} = R_{C-} = 0$, we obtain $V_C = -V_{bias}^2/V_G$, which corresponds to the result of the input electrode capacitor model [6], [7] and indicates a symmetric $V_C - V_{bias}$ curve as shown in Fig. 1(b). Eq. (3) clearly shows that the symmetry of the $V_C - V_{bias}$ curve is broken by the right second term, when the input contact resistances are not the same. Since the right second term is proportional to V_{bias}, the parabolic V_C curve simply inclines when $R_{C-} \neq R_{C+}$.

3. Comparison with Experiment

Next we investigate the validity of the model and clarify the effect of the contact resistance inequality by comparison with experimentally obtained characteristics in the fabricated graphene TBJ. A graphene sheet was obtained by micromechanical exfoliating graphite and it was transferred on a 90-nm silicon oxide substrate. The monolayer was determined by optical contrast [10]. Metal electrode patterns were formed by electron beam lithography, and 40 nm PtPd alloy was deposited by sputtering and lift-off. In our experiment, PtPd alloy often showed poor ohmic contact with large variation of resistivity from $4 \times 10^{-5}\,\Omega\text{cm}^2$ to $4 \times 10^{-4}\,\Omega\text{cm}^2$. A T-shape TBJ structure was formed by electron-beam lithography and oxygen plasma etching. In order to shift V_{CNP} to 0 V, the sample was immersed in polyethylenimine (PEI) for 24 h [11]. All the measurements carried out at room temperature. Figure 3 shows the measured branch resistances as function of V_G in the fabricated TBJ device. R_{total} was evaluated from the current-voltage, $I_{total} - V_{bias}$, characteristic through the two input branches, which included the graphene branch resistances

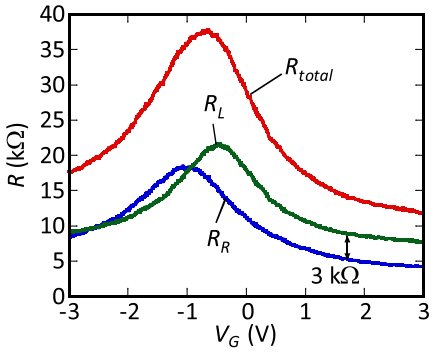

Fig. 3 Measured resistances of the input branches.

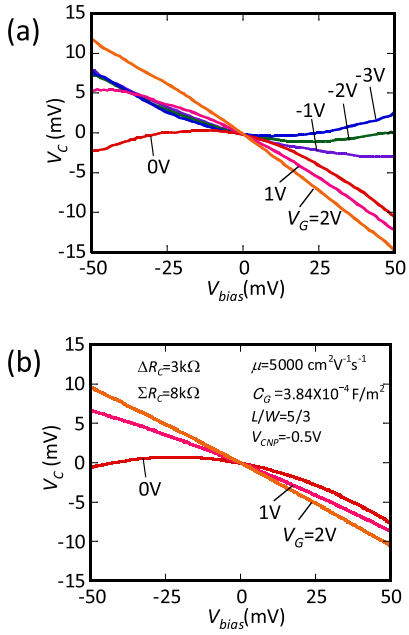

Fig. 4 Nonlinear voltage transfer characteristics of a graphene TBJ: (a) Experiment and (b) theory.

and the metal-graphene contact resistances in the two inputs. Here V_{bias} was applied in push–pull fashion. In this measurement, V_C was also monitored. Then the left and right branch resistances, R_L and R_R, respectively, were evaluated by $R_L = (V_{bias} - V_C)/I_{total}$ and $R_R = (V_C + V_{bias})/I_{total}$, respectively. Evaluated R_L included the graphene branch resistance and the metal-graphene contact resistance only in the left input branch. As V_G increased, both R_L and R_R decreased rapidly and saturated. This saturation arose from the contact resistance, since the graphene resistance was sufficiently low. Taking account of this point, observed resistance difference of 3 kΩ between left and right branch resistances in Fig. 3 was considered to be $\Delta R_C = R_{C+} - R_{C-}$ for electrons. Unfortunately, we could not estimate ΔR_C for hole, because the current saturation was not observed when $V_G \ll 0$ in this experiment.

Figure 4 compares the experimental and theoretical $V_C - V_{bias}$ curves of the graphene TBJ. Theoretical curves are shown for electrons only, because ΔR_C for hole could

not be obtained from Fig. 3. The experimental curves obviously inclined and the slope of the incline depended on V_G. Using $\Delta R_C = 3\,k\Omega$ for electrons together with other experimentally obtained parameters, $\mu = 5{,}000\,cm^2/Vs$, $C_G = 3.84 \times 10^{-4}\,F/m^2$, $L/W = 500\,nm/300\,nm$, $V_{CNP} = -0.5\,V$, and $\Sigma R_C = R_{C+} + R_{C-} = 8\,k\Omega$, the asymmetric nonlinear characteristics in the fabricated device could be reproduced by Eq. (3) very well. This result verified the validity of our model for explaining the non-ideal nonlinear curves. It was found that unequal input contact resistances gave a significant impact on nonlinear voltage transfer curve in the TBJ. Formation of low and uniform metal-graphene contacts is necessary for achieving an ideal voltage transfer characteristic.

4. Impact of Improved Metal-Graphene Contacts

In order to obtain reduced metal-graphene contact resistance reproducibly, we investigated the Ni/Au stack for the metal electrodes. This metal stack is known to provide a low contact resistivity for graphene [9], [12], [13]. In this experiment, the graphene surface was cleaned by annealing at 300°C for 1 h prior to the lithography. Then the metal electrode patterns were formed by electron beam lithography. 10-nm Ni/50-nm Au was deposited via electron beam evaporation and lift-off. Using a cross bridge Kelvin method [9], the Ni/Au electrodes were found to achieve $5\times10^{-6}\ \Omega cm^2$ in the high carrier density regime, which was comparable to the other reported values [9]. This resistance was much lower than that of the PtPd alloy.

We fabricated the graphene TBJ device with the improved metal-graphene contact formation process. Figure 5(a) shows AFM phase image of the fabricated graphene TBJ. It could show the configuration of the device even covered with a thick PEI layer for surface doping. Each branch had a length of 500 nm and a width of 300 nm. Figure 5(b) shows the measured resistance thorough the input branches. The resistance was evaluated from the current through the two input branches by applying voltage of 0.1 V. Obviously smaller resistance value than the previous device was obtained. Estimated sum of the contact resistances in the two input electrodes was 100 Ω, which was 80 times smaller than that in the previous device. In this plot, we found $V_{CNP} = -1\,V$, however, it was sensitive to the environment and often shifted slightly. Estimated effective electric field mobility was $5{,}000\,cm^2\ V^{-1}s^{-1}$.

Figure 6 shows the measured voltage transfer characteristic of the fabricated device with the improved contact formation process. The curves showed clear parabolic curves without incline. They were well controlled by V_G. The polarity of the curves was switched between $V_G = 1\,V$ and 2 V owing to the change of conduction type. A slight asymmetry was observed in the curve at $V_G = 2\,V$. Considering that the device was geometrically symmetric as shown in Fig. 5(a) and the asymmetric curve only appeared near the charge neutral point, the observed asymmetry was attributed by a small difference of the charge neutrality point between

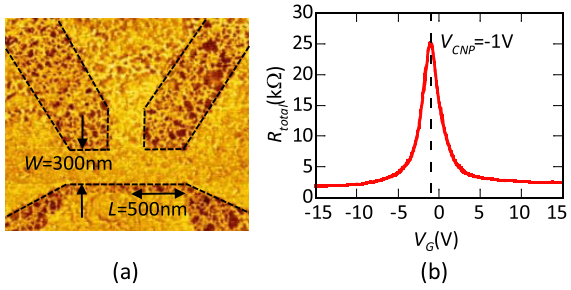

Fig. 5 (a) AFM phase image of the fabricated TBJ device using optimized contact formation process and (b) measured resistance value through the two inputs.

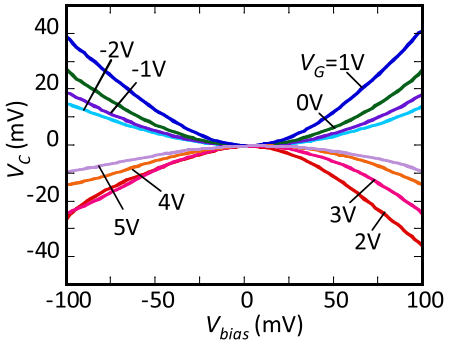

Fig. 6 Measured voltage transfer characteristics in the fabricated TBJ with improved metal-graphene contacts.

the two input branches. Assuming the contact resistance of 0 for simplicity, we obtained the following equation for V_C from Eqs. (1) and (2),

$$V_C = -\frac{1}{V_G - \overline{V_{CNP}}} V_{bias}^2 + \frac{\Delta V_{CNP}}{2\left(V_G - \overline{V_{CNP}}\right)} V_{bias}, \tag{4}$$

where $\overline{V_{CNP}}$ and ΔV_{CNP} are average and difference of the charge neutrality points of the left and right branches, respectively. This equation indicates that the curve inclines as V_G approaches $\overline{V_{CNP}}$ when ΔV_{CNP} is non-zero. Variation of V_{CNP} might arise from inhomogeneous charge distribution by PEI doping.

We evaluated the symmetry of the measured voltage transfer curves in the fabricated devices with and without the improved contacts. The result is shown in Fig. 7. Here the symmetry, β, was defined as follows:

$$\beta = \frac{|V_C(V_{bias}) - V_C(-V_{bias})|}{2|V_{bias}|}. \tag{5}$$

The values of V_{bias} for the devices with and without improved contacts were 100 mV and 50 mV, respectively. The clear difference was observed between the two devices. Theoretical β is found to be the coefficient of V_{bias} term in Eq. (3). The calculated curves are also shown in Fig. 7, which could explain the experimental curves reasonably well. In the device without the improved contact, β was monotonically increased as V_G increased and reached as high as 30%.

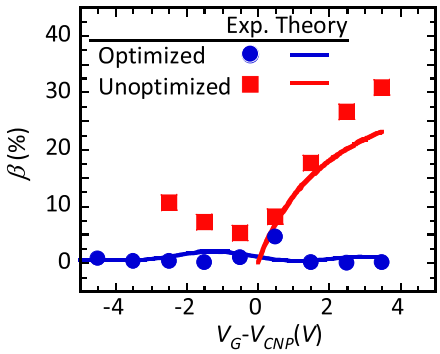

Fig. 7 Comparison of transfer curve symmetry in the two fabricated graphene TBJs. Theoretical curves from Eq. (3) are also plotted.

On the other hand, β from the device with the improved contact was very small and less than 2% was achieved even at $V_G - V_{CNP} = 4$ V. Obtained results clarified a large impact of the uniformity of the metal-graphene contact resistance on the graphene TBJ nonlinear characteristics.

5. Conclusions

We investigated the origin of the non-ideal transfer characteristics in graphene-based three-branch nano-junction (TBJ) device. A simple model considering the contact resistances in two input electrodes was deduced and it could explain the observed behaviors well. The model analysis suggested that the non-ideal characteristic arose from the inequality in the metal-graphene contact resistances of the input branches. We fabricated the graphene TBJ device with almost equal metal-graphene contacts by optimizing the formation process. The fabricated device with the improved contact successfully showed almost ideal nonlinear characteristic.

Acknowledgments

We thank Prof. S. W. Hwang and Prof. D. M. Wang for providing materials. This work was partly supported by Grant-in-Aid for Scientific Research on Innovative Areas “Molecular Architectonics: Orchestration of Single Molecules for Novel Functions.”

References

[1] H. Q. Xu, “Electrical properties of three-terminal ballistic junctions,” Appl. Phys. Lett., vol.78, no.14, pp.2064–2066, Apr. 2001.
[2] L. Worschech, A. Schliemann, S. Reitzenstein, P. Hartmann, and A. Forchel, “Microwave rectification in ballistic nanojunctions at room temperature,” Microelectron. Eng., vol.63, no.1–3, pp.217–221, Aug. 2002.
[3] S. F. B. A. Rahman, D. Nakata, Y. Shiratori, and S. Kasai, “Boolean logic gates utilizing GaAs three-branch nanowire junctions controlled by Schottky wrap gates,” Jpn. J. Appl. Phys., vol.48, no.6S, p.06FD01, June 2009.
[4] A. Jacobsen, I. Shorubalko, L. Maag, U. Sennhauser, and K. Ensslin, “Rectification in three-terminal graphene junctions,” Appl. Phys. Lett., vol.97, no.3, p.032110, July 2010.
[5] S. F. A. Rahman, S. Kasai, A. M. Hashim, and V. K. Arora, “Fabrication and characterization of graphene-based three-branch nanojunction device,” Digest of Asia-Pacific Workshop on Fundamentals and Applications of Advanced Semiconductor Devices (AWAD2012), Daejan, Korea, June 29–July 1, 2011.
[6] X. Yin and S. Kasai, “Graphene-based three-branch nano-junction (TBJ) logic inverter,” Phys. Status Solidi C, vol.10, no.11, pp.1485–1488, Nov. 2013.
[7] S. F. A. Rahman, S. Kasai, and A. M. Hashim, “Room temperature nonlinear operation of a graphene-based three-branch nanojunction device with chemical doping,” Appl. Phys. Lett., vol.100, no.19, p.193116, May 2012.
[8] R. J. Zhu, Y. Q. Huang, N. Kang, and H. Q. Xu, “Gate tunable nonlinear rectification effects in three-terminal graphene nanojunctions,” Nanoscale, vol.6, no.9, pp.4527–4531, May 2014.
[9] K. Nagashio, T. Nishimura, K. Kita, and A. Toriumi, “Contact resistivity and current flow path at metal/graphene contact,” Appl. Phys. Lett., vol.97, no.14, p.143514, Oct. 2010.
[10] S. F. A. Rahman, A. M. Hashim, and S. Kasai, “Identification of graphene layer numbers from color combination contrast image for wide-area characterization,” Jpn. J. Appl. Phys., vol.51, no.6S, p.06FD09, June 2012.
[11] D. B. Farmer, R. Golizadeh-Mojarad, V. Perebeinos, Y.-M. Lin, G. S. Tulevski, J. C. Tsang, and P. Avouris, “Chemical doping and electron-hole conduction asymmetry in graphene devices,” Nano Lett., vol.9, no.1, pp.388–392, Jan. 2009.
[12] J. A. Robinson, M. LaBella, M. Zhu, M. Hollander, R. Kasarda, Z. Hughes, K. Trumbull, R. Cavalero, and D. Snyder, “Contacting graphene,” Appl. Phys. Lett., vol.98, no.5, p.053103, Jan. 2011.
[13] E. Watanabe, A. Conwill, D. Tsuya, and Y. Koide, “Low contact resistance metals for graphene based devices,” Diam. Relat. Mater., vol.24, pp.171–174, Apr. 2012.

Xiang Yin received the B.E. degree in microelectronics at Southwest Jiaotong University, China in 2010. Then he joined the Graduate School of Information Science and Technology, Hokkaido University, Japan in 2011 and received his M.E. degree in 2013. He is continuing for his Ph.D. degree. His current research interests focus on graphene nanodevice. He is a member of the Japan Society of Applied Physics.

Masaki Sato received B.E. degree in electronics and information engineering and M.S. degree in information science and technology from Hokkaido University, Sapporo, Japan, in 2011 and 2013, respectively. He is continuing research for Ph.D. degree. He is engaged in research on GaAs-based electron devices. He is a member of the Japan Society of Applied Physics, and the Institute of Electronics, Information and Communication Engineers.

Seiya Kasai received B.E., M.E. and Ph.D. degrees in electrical engineering from Hokkaido University, Hokkaido, Japan, in 1992, 1994 and 1997, respectively. He joined Optoelectronics and High Frequency Device Research Laboratories, NEC, Japan, in 1997. In 1999, he moved to Graduate School of Electronics and Information Engineering, Hokkaido University, as a Research Associate and he has been an Associate Professor since 2001. From 2014, he has been a Professor in Research Center for Integrated Quantum Electronics (RCIQE), Hokkaido University. His current research interests include semiconductor nanodevices and their integrations, and bio-inspired electron devices and systems. He is a member of IEEE, the Institute of Electronics, Information and Communication Engineers (IEICE), and the Japan Society of Applied Physics (JSAP).